Electronic supplementary information

Newly synthesized palladium(II) complexes with aminothiazole derivatives: *In vitro* study of antimicrobial activity and antitumor activity on human prostate cancer cell line

Dejan Simić[a], Milan Zarić[b], Ivana Nikolić[b], Radica Zivković-Zarić[c], Petar Čanović[b], Aleksandar Kočović[d], Ivana Radojević[e], Ivana Raković[f], Sandra Jovičić Milić[g], Đorđe Petrović[g], Danijela Stojković[h], Nenad Vuković[g], Miroslava Kačániová[i], Milena Vukić[g], Verica Jevtić[g]

[a]University of Defence, Belgrade, Serbia, Military Medical Academy, Department of Urology, Crnotravska 17, 11040 Belgrade, Serbia.
[b]University of Kragujevac, Serbia, Faculty of Medical Sciences, Department of Biochemistry, Svetozara Markovica 69, 34000 Kragujevac, Serbia.
[c]University of Kragujevac, Serbia, Faculty of Medical Sciences, Department of Pharmacology and Toxicology, Svetozara Markovica 69, 34000 Kragujevac, Serbia.
[d]University of Kragujevac, Serbia, Faculty of Medical Sciences, Department of Pharmacy, Svetozara Markovica 69, 34000 Kragujevac, Serbia.
[e]University of Kragujevac, Serbia, Faculty of Science, Department of Biology, Radoja Domanovica 12, 34000 Kragujevac, Serbia.
[f]University of Kragujevac, Serbia, Faculty of Medical Sciences, Department of Infectious diseases, Svetozara Markovica 69, 34000 Kragujevac, Serbia.
[g]University of Kragujevac, Serbia, Faculty of Science, Department of Chemistry, Radoja Domanovica 12, 34000 Kragujevac, Serbia.
[h]University of Kragujevac, Serbia, Institute for Information Technologies, Jovana Cvijica bb, 34000 Kragujevac, Serbia.
[i]Slovak University of Agriculture, Faculty of Horticulture and Landscape Engineering, Department of Fruit sciences, Viticulture and Enology, Trieda Andreja Hlinku 2, 949 76 Nitra-Chrenová, Slovakia.

IR SPECTRAL ANALYSIS

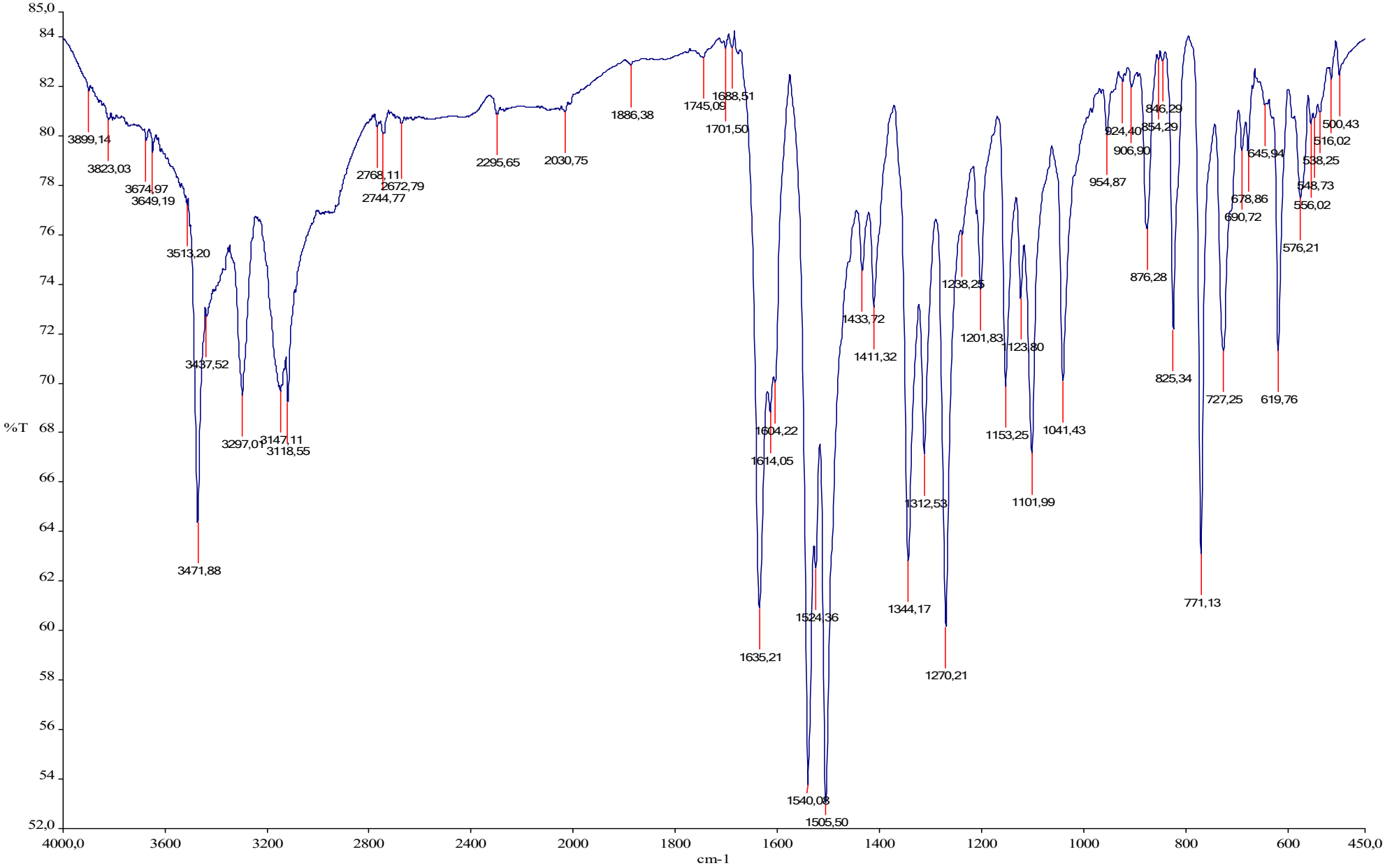

Figure S1. IR spectrum of L1

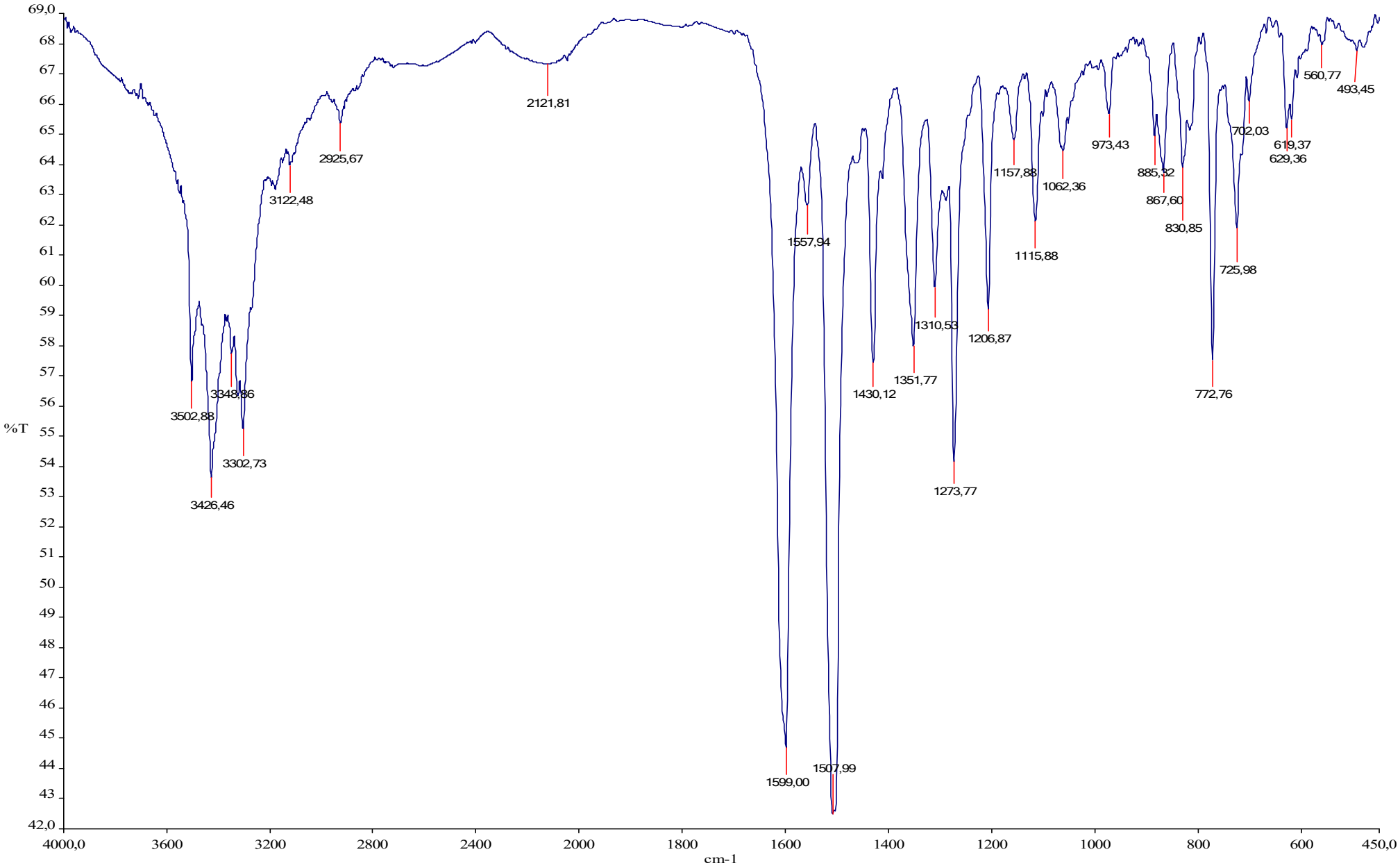

Figure S2. IR spectrum of C1

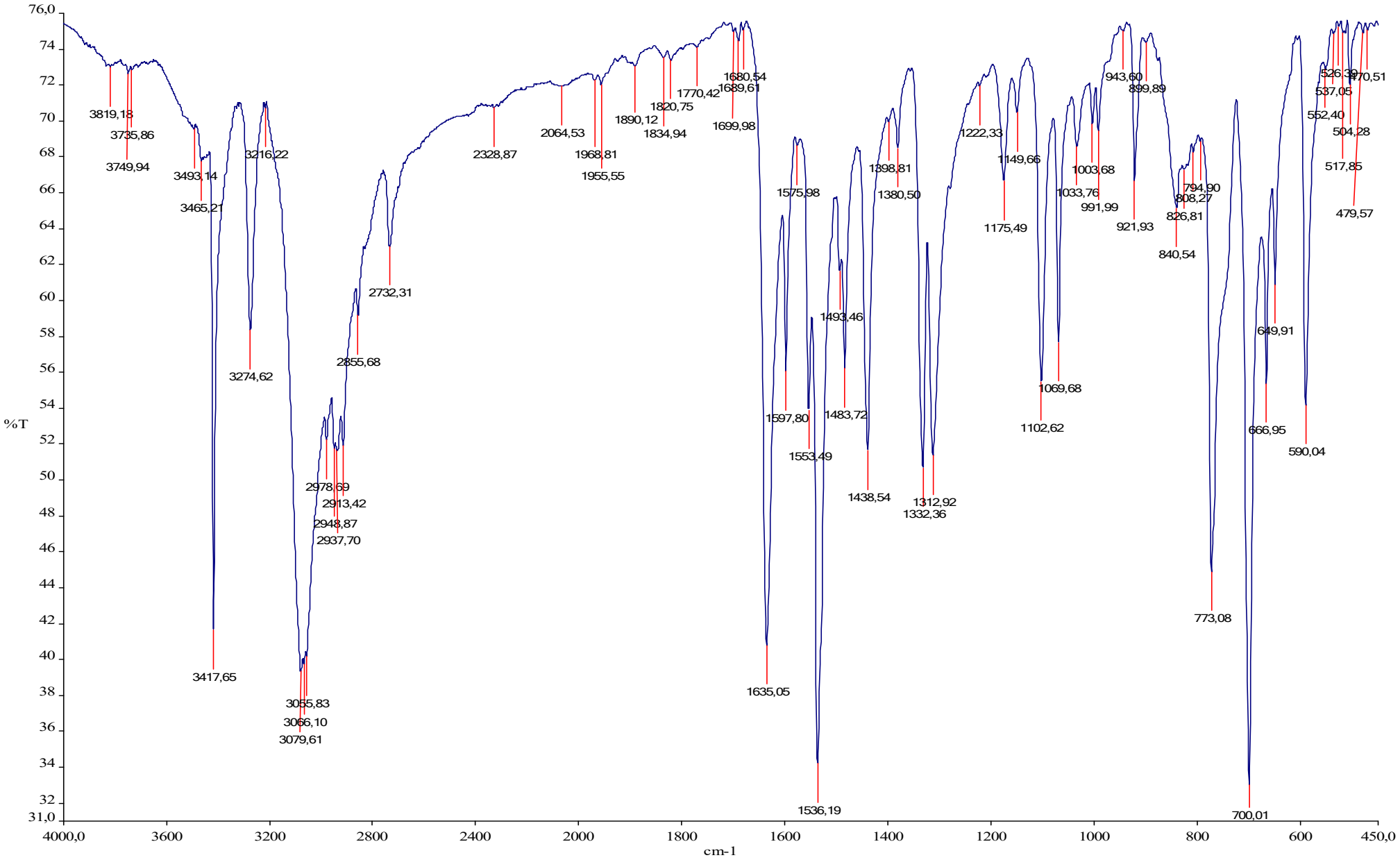

Figure S3. IR spectrum of L2

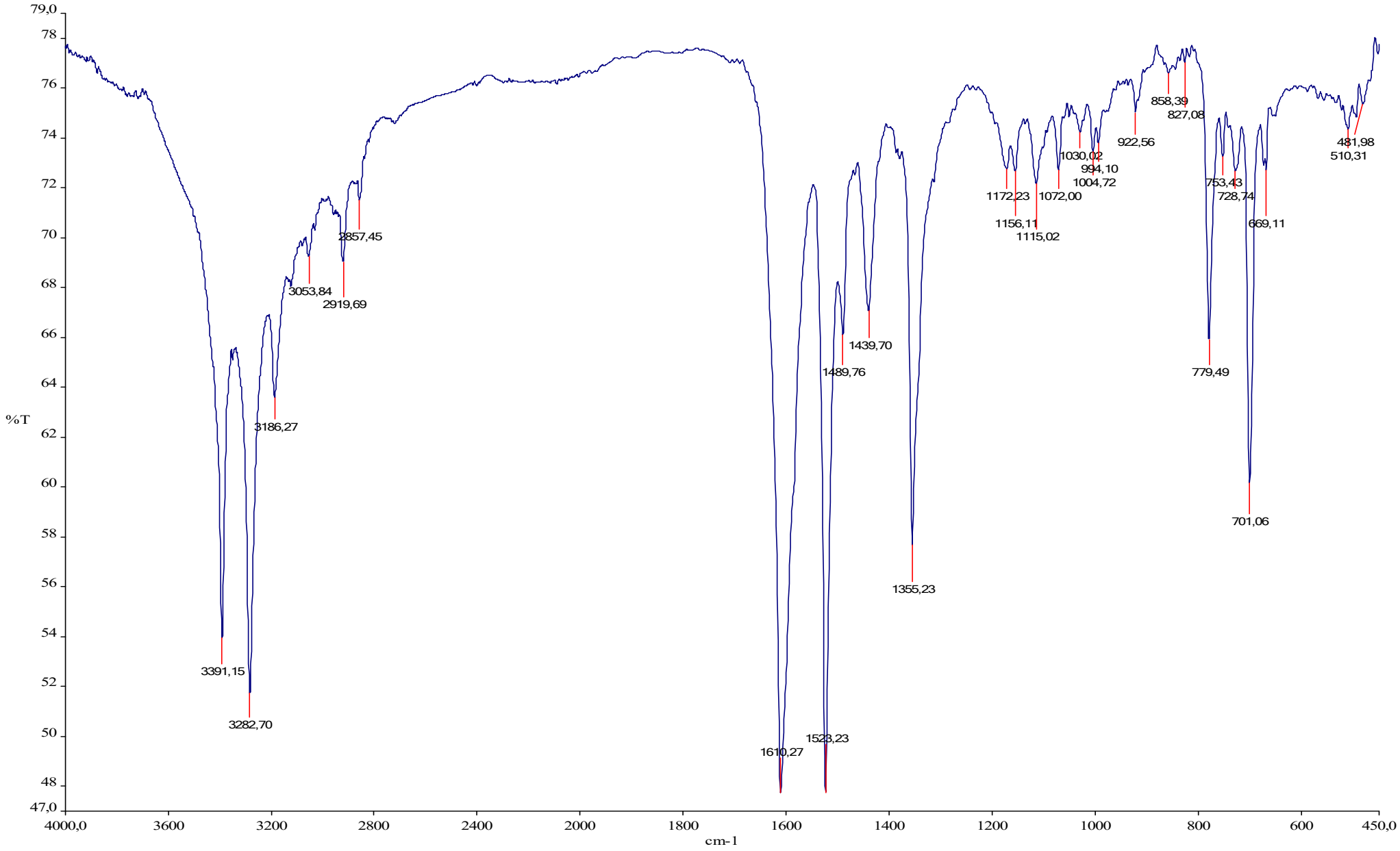

Figure S4. IR spectrum of C2

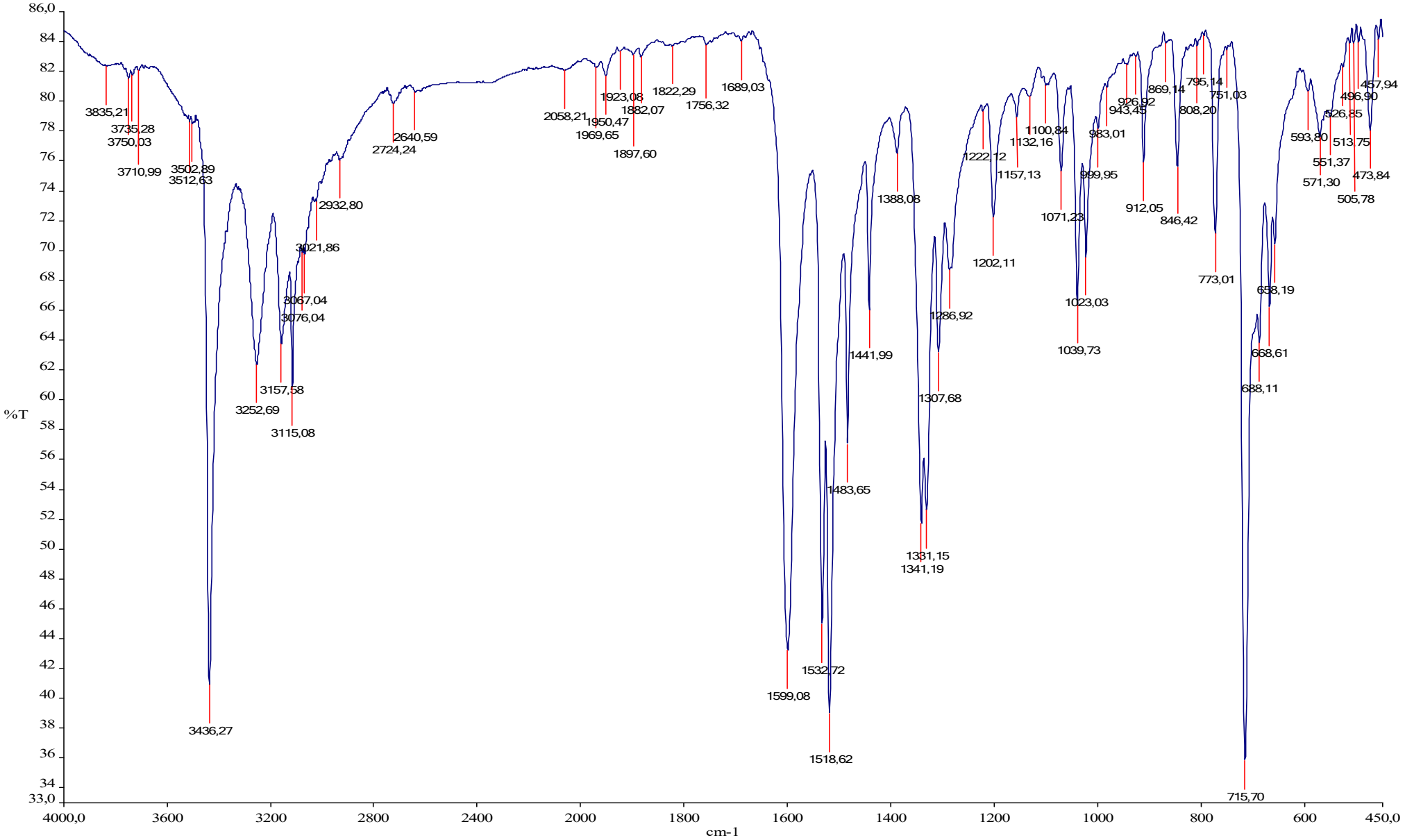

Figure S5. IR spectrum of L3

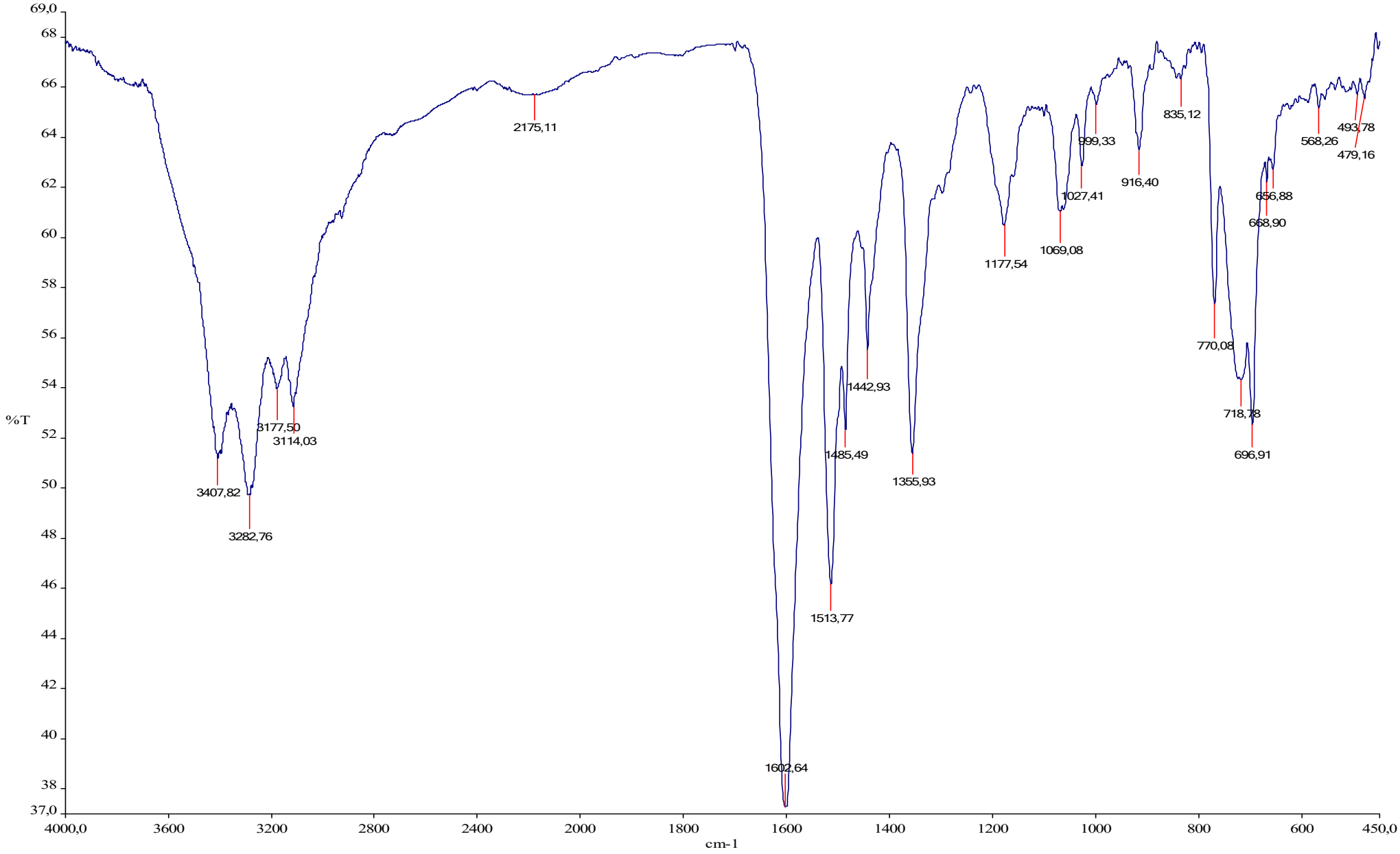

Figure S6. IR spectrum of C3

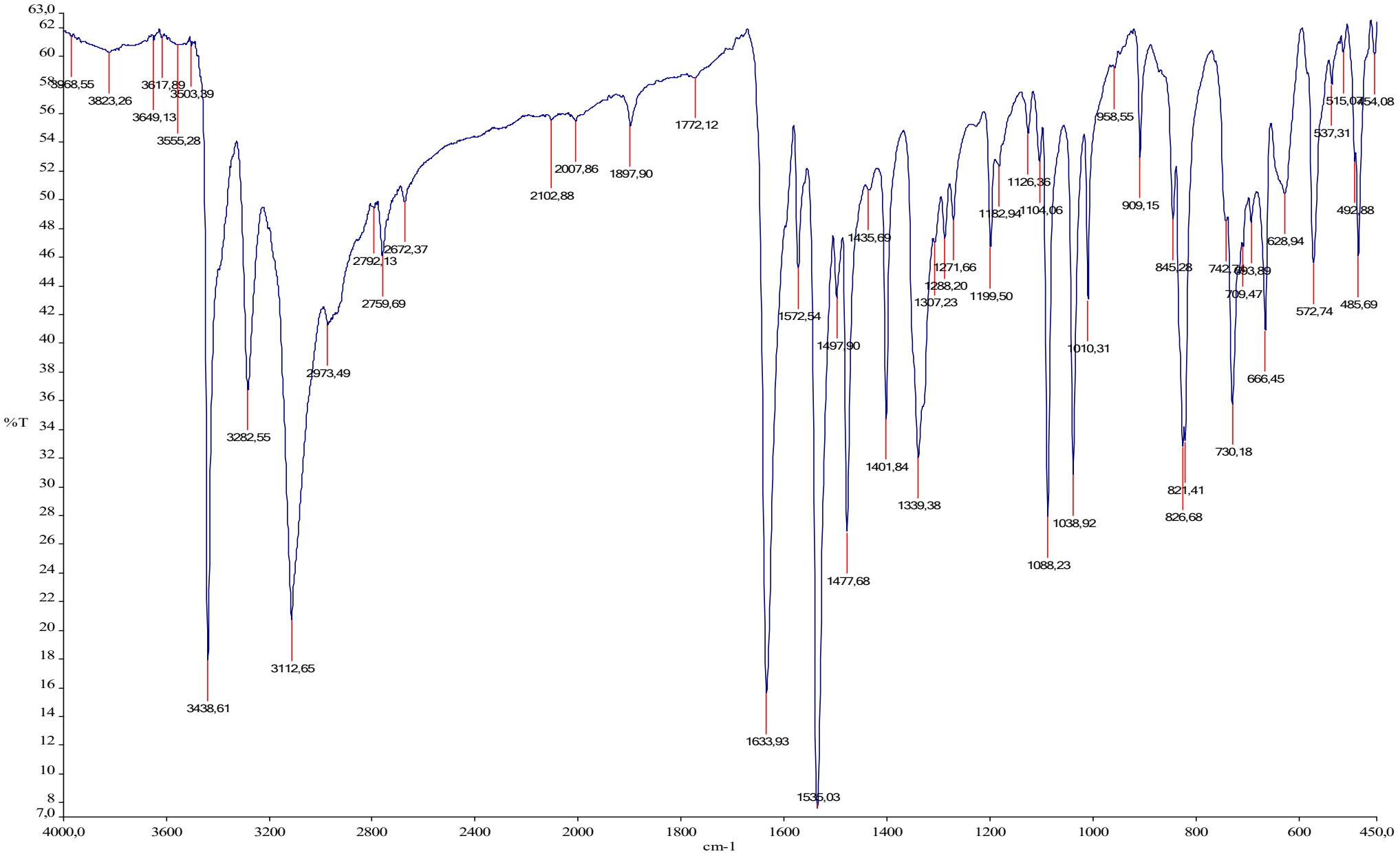

Figure S7. IR spectrum of L4

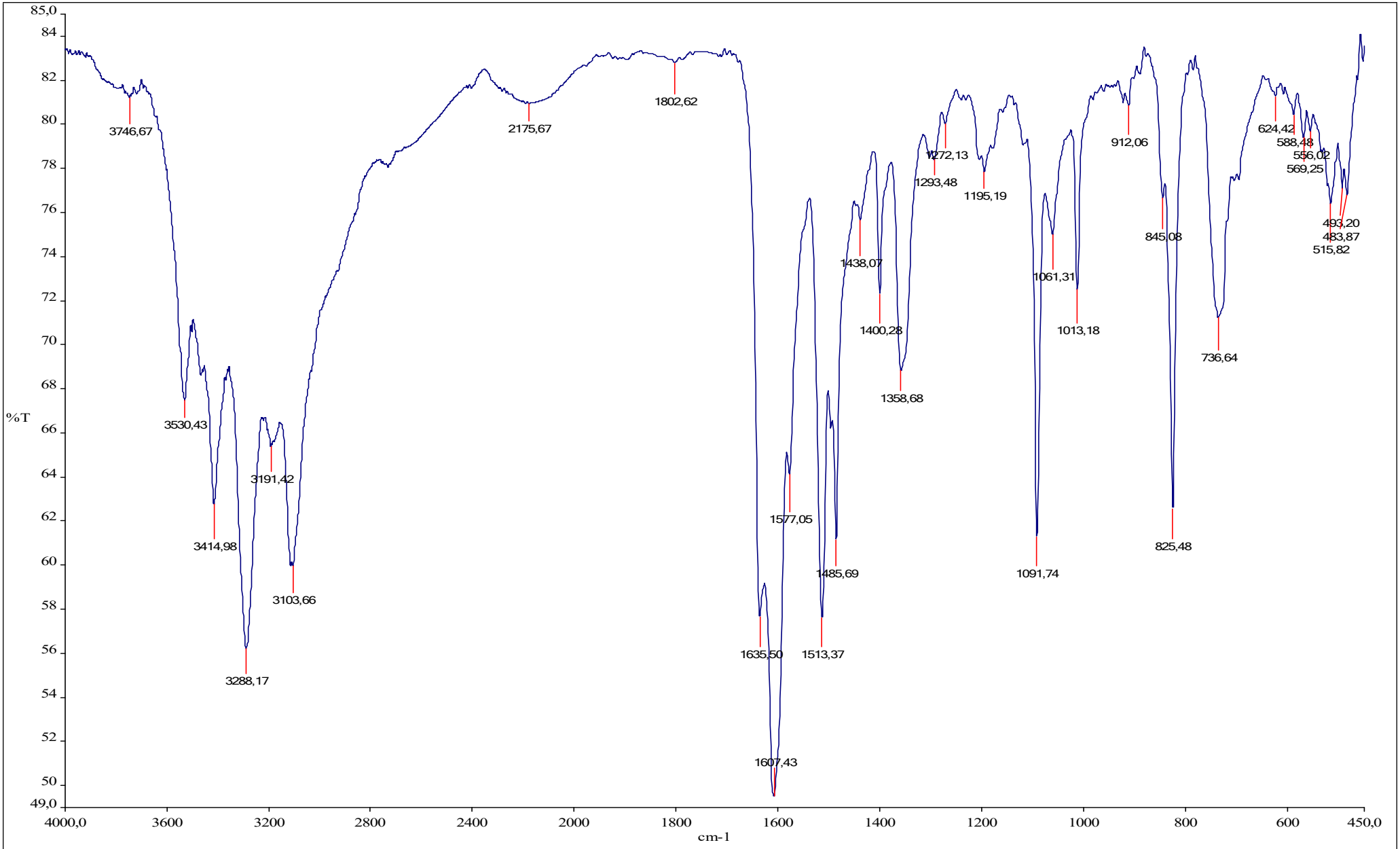

Figure S8. IR spectrum of C4

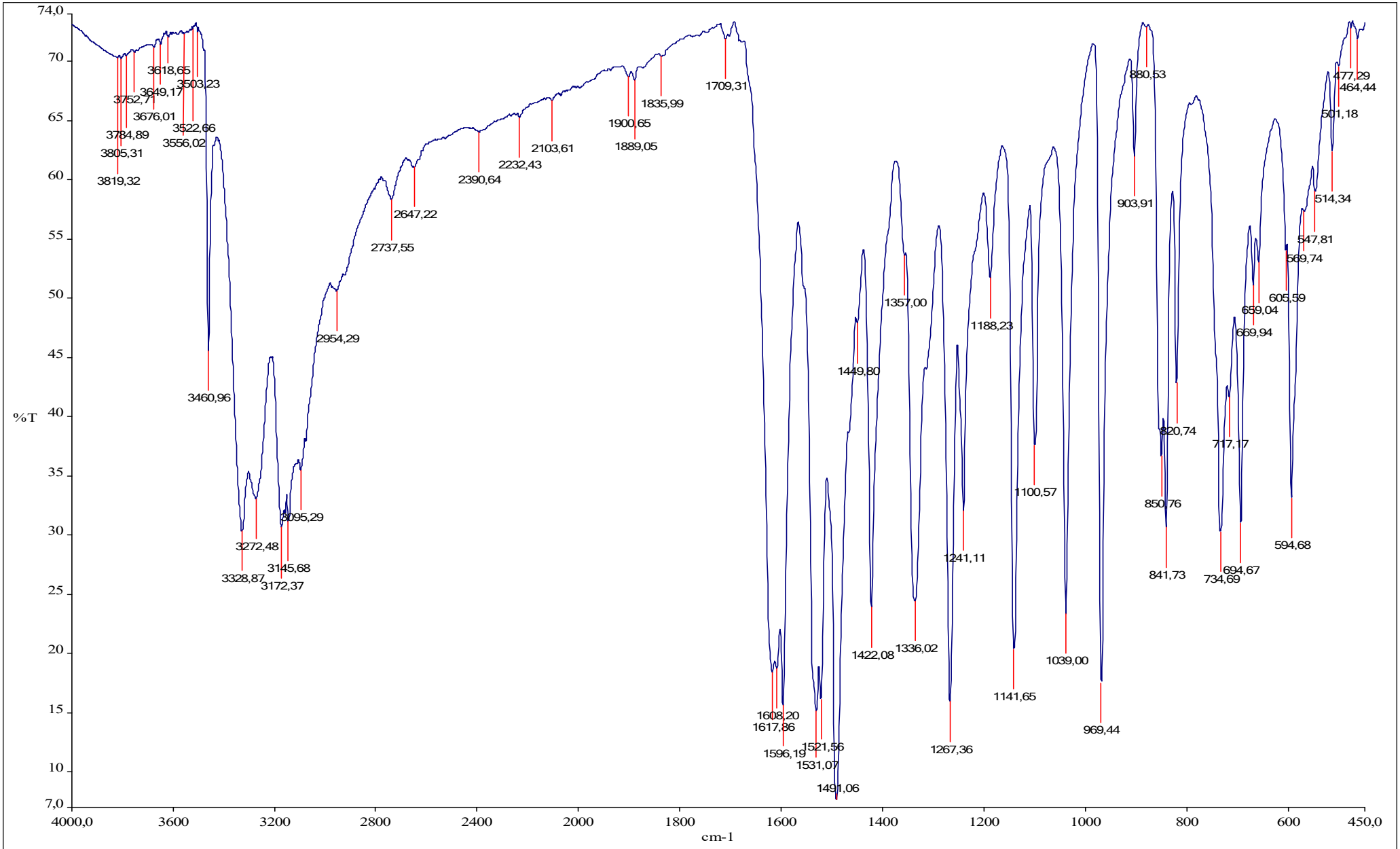

Figure S9. IR spectrum of L5

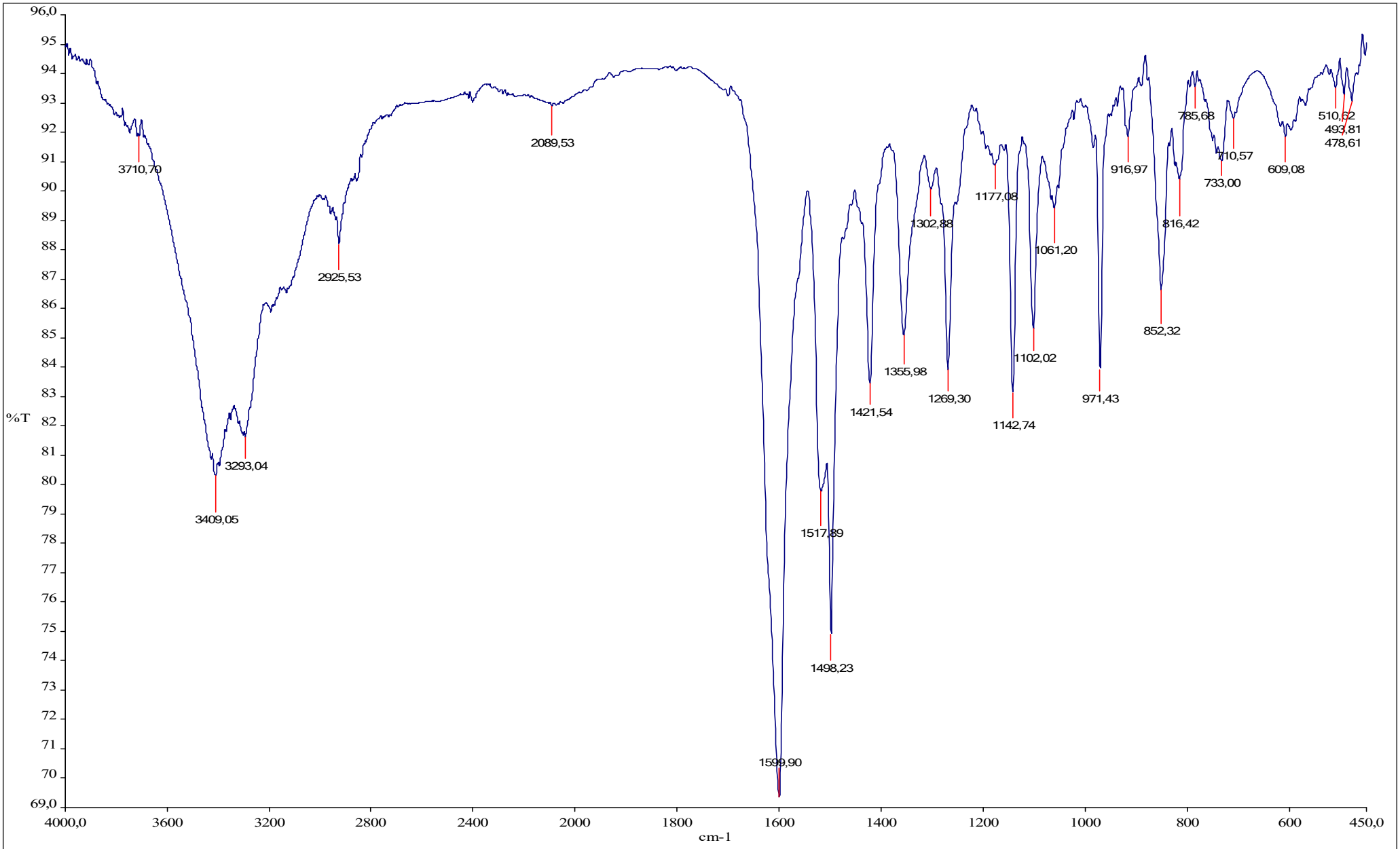

Figure S10. IR spectrum of C5

COMPLEX STABILITY

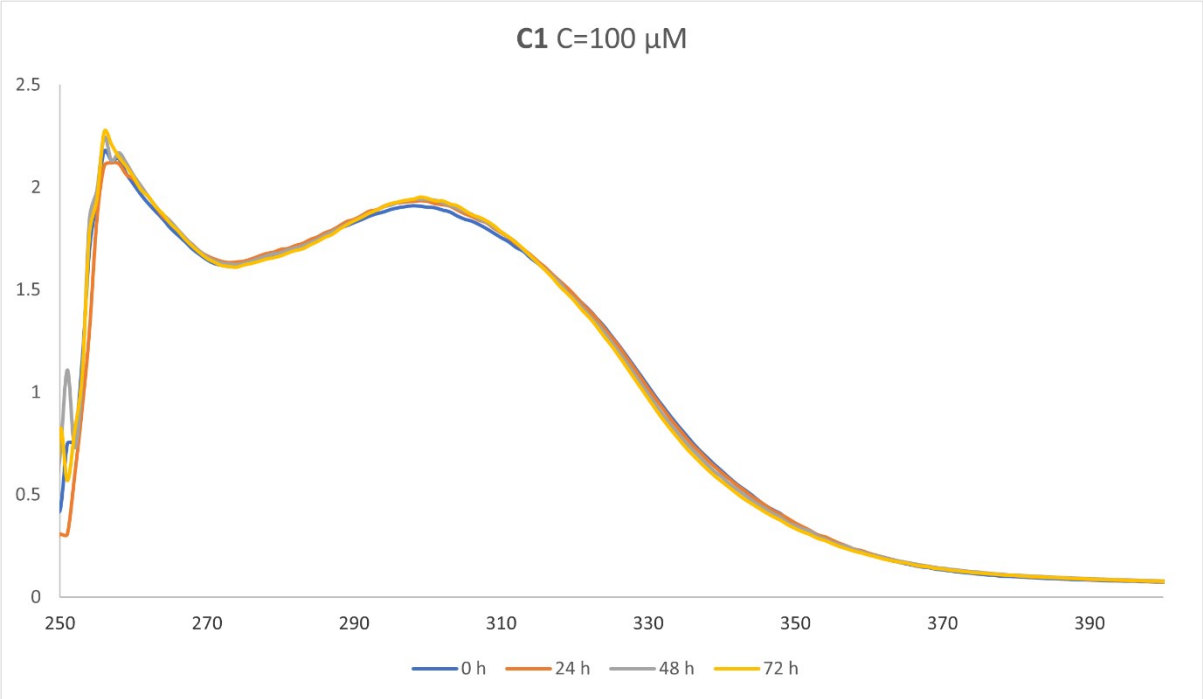

Figure S11. UV-Vis spectrum of C1 [100 µM] in 5% DMSO immediately after dissolving and 24, 48 and 72 h after dissolving

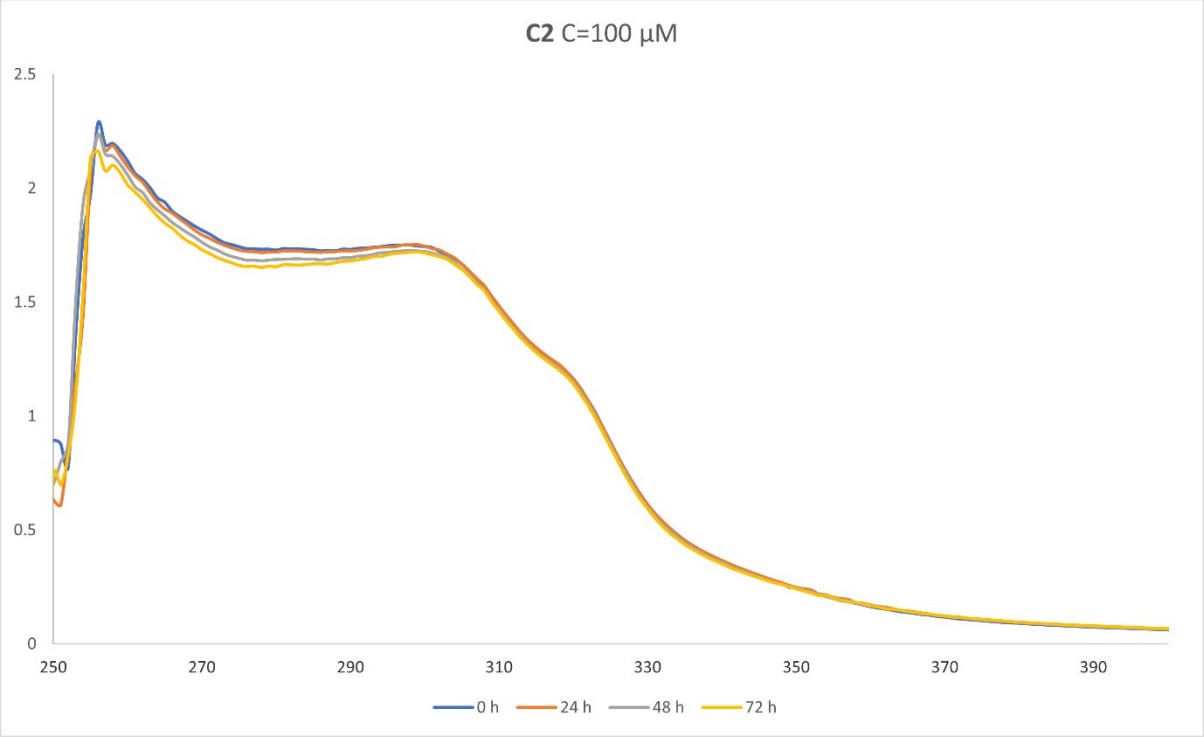

Figure S12. UV-Vis spectrum of C2 [100 µM] in 5% DMSO immediately after dissolving and 24, 48 and 72 h after dissolving

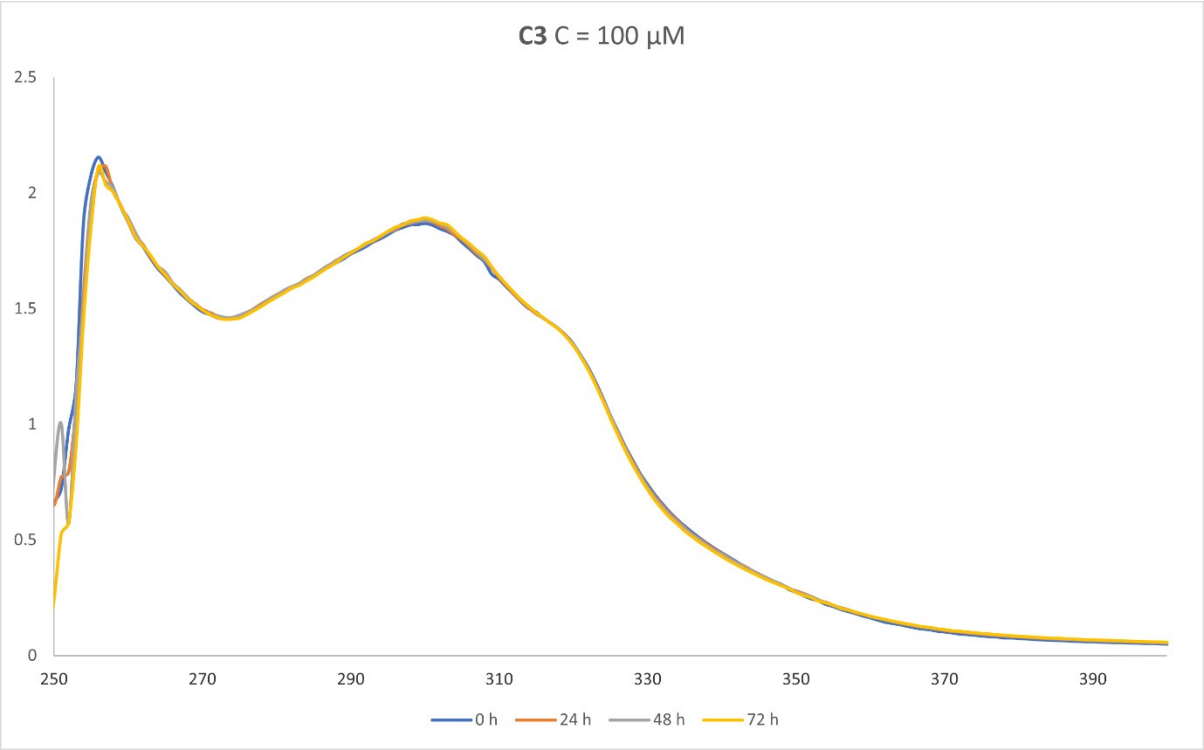

Figure S13. UV-Vis spectrum of C2 [100 µM] in 5% DMSO immediately after dissolving and 24, 48 and 72 h after dissolving

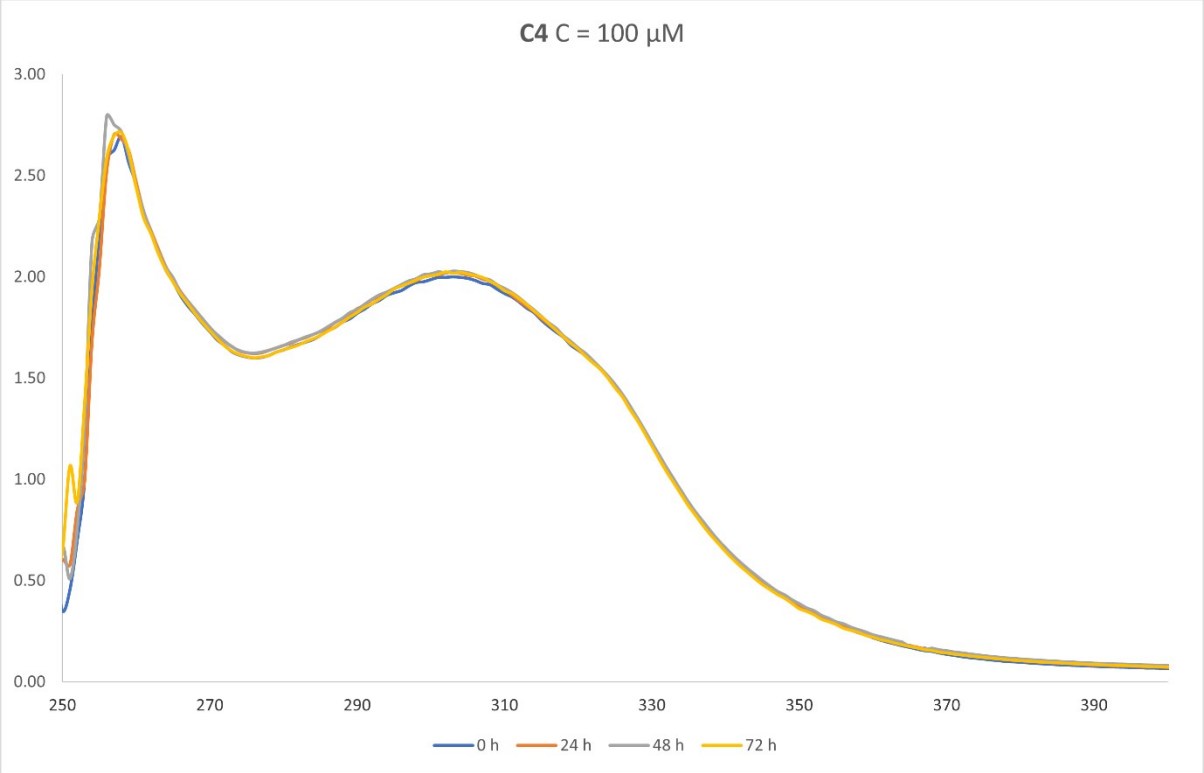

Figure S14. UV-Vis spectrum of C2 [100 µM] in 5% DMSO immediately after dissolving and 24, 48 and 72 h after dissolving

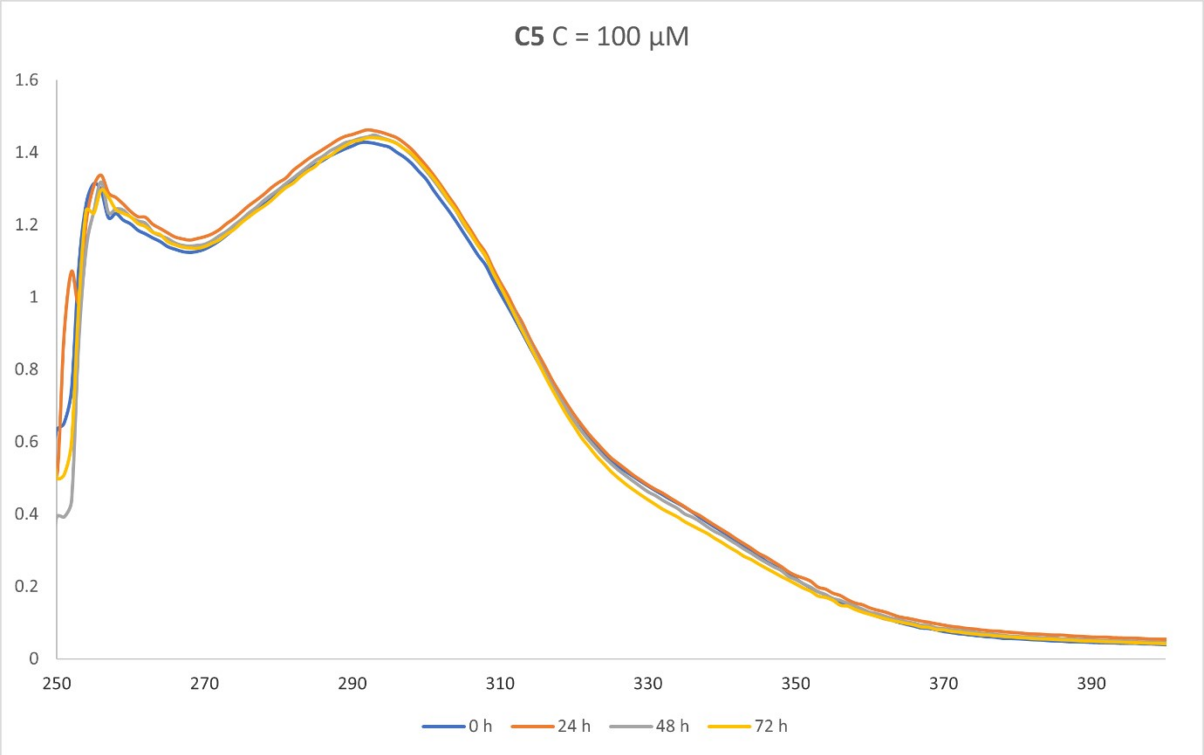

Figure S15. UV-Vis spectrum of C2 [100 µM] in 5% DMSO immediately after dissolving and 24, 48 and 72 h after dissolving

INTERACTION OF COMPLEXES WITH DNA

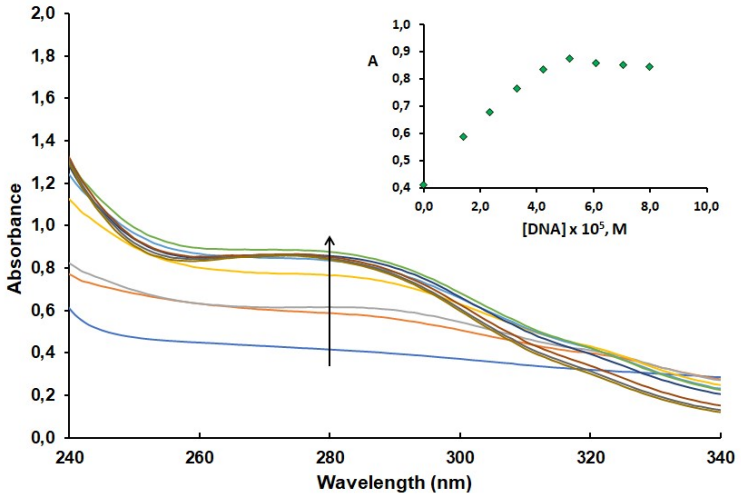

Figure S16. Absorption spectra of complex C2 at room temperature in PBS buffer upon the addition of CT-DNA. [complex] = 5.0 × 10^{-5} mol dm^{-3}, [DNA] = 0–8.4×10^{-5} mol dm^{-3}. The arrow shows the change of absorbance with the increase of DNA concentration. Inset: plot of the absorption data at 280 nm, demonstrating the saturation of binding of complex **C2** to CT-DNA.

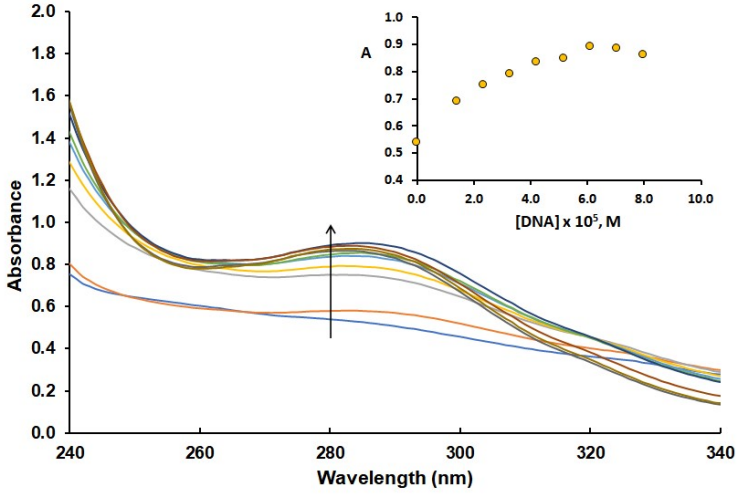

Figure S17. Absorption spectra of complex C3 at room temperature in PBS buffer upon the addition of CT-DNA. [complex] = 5.0 × 10^{-5} mol dm^{-3}, [DNA] = 0–8.4×10^{-5} mol dm^{-3}. The arrow shows the change of absorbance with the increase of DNA concentration. Inset: plot of the absorption data at 280 nm, demonstrating the saturation of binding of complex **C3** to CT-DNA.

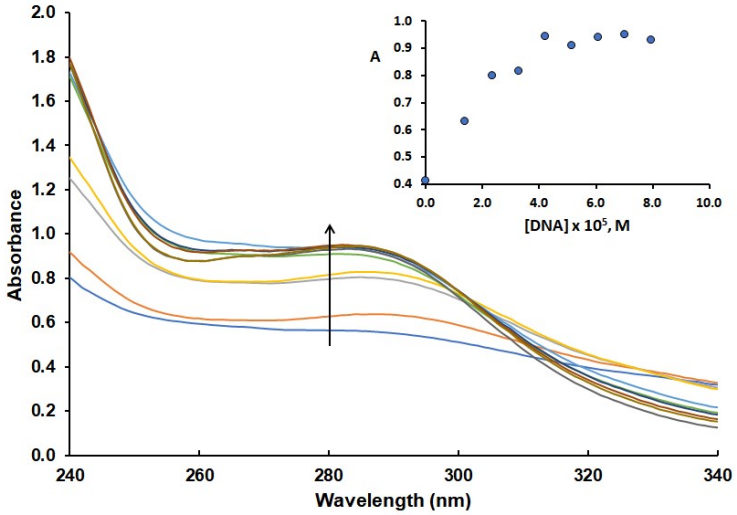

Figure S18. Absorption spectra of complex C4 at room temperature in PBS buffer upon the addition of CT-DNA. [complex] = 5.0 × 10^{-5} mol dm^{-3}, [DNA] = 0–8.4×10^{-5} mol dm^{-3}. The arrow shows the change of absorbance with the increase of DNA concentration. Inset: plot of the absorption data at 280 nm, demonstrating the saturation of binding of complex **C4** to CT-DNA.

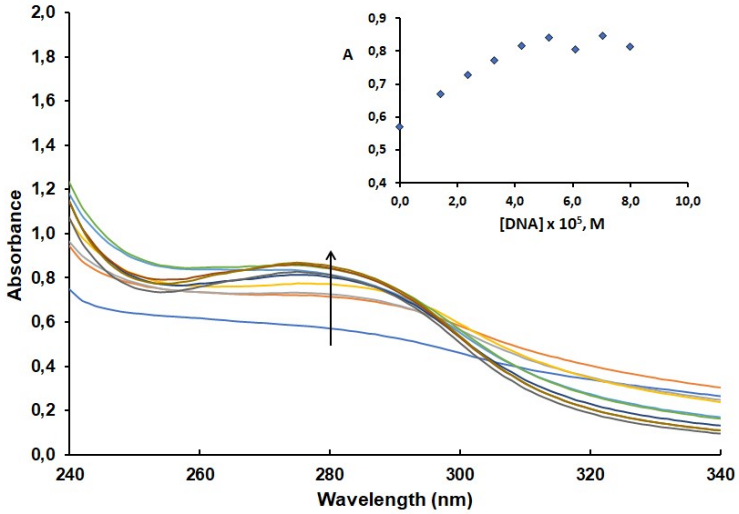

Figure S19. Absorption spectra of complex C5 at room temperature in PBS buffer upon the addition of CT-DNA. [complex] = 5.0 × 10^{-5} mol dm^{-3}, [DNA] = 0–8.4×10^{-5} mol dm^{-3}. The arrow shows the change of absorbance with the increase of DNA concentration. Inset: plot of the absorption data at 280 nm, demonstrating the saturation of binding of complex **C5** to CT-DNA.

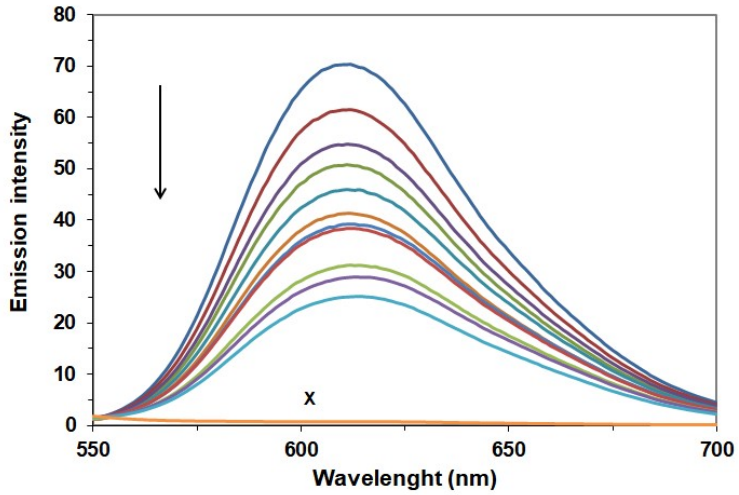

Figure S20. Emission spectra of EB bound to DNA in the presence of complex **C2**. [EB] = 2.0×10^{-5} mol dm^{-3}; [DNA] = 2.35×10^{-3} mol dm^{-3}; [complex] = 0-3.6×10^{-5} mol dm^{-3}; λ_{ex} = 520 nm. Arrow shows the emission intensity changes upon increasing complex concentration. **x** represents 3.6×10^{-5} mol dm^{-3} complex only.

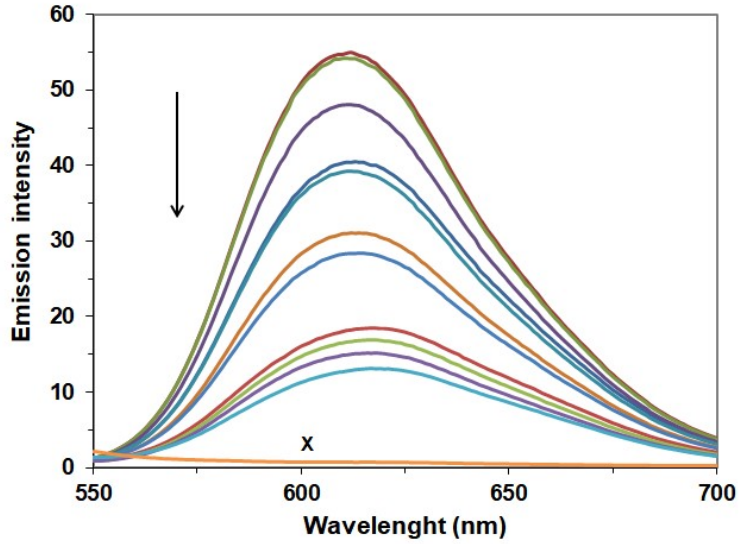

Figure 21. Emission spectra of EB bound to DNA in the presence of complex **C3**. [EB] = 2.0×10^{-5} mol dm^{-3}; [DNA] = 2.35×10^{-3} mol dm^{-3}; [complex] = 0-3.6×10^{-5} mol dm^{-3}; λ_{ex} = 520 nm. Arrow shows the emission intensity changes upon increasing complex concentration. **x** represents 3.6×10^{-5} mol dm^{-3} complex only.

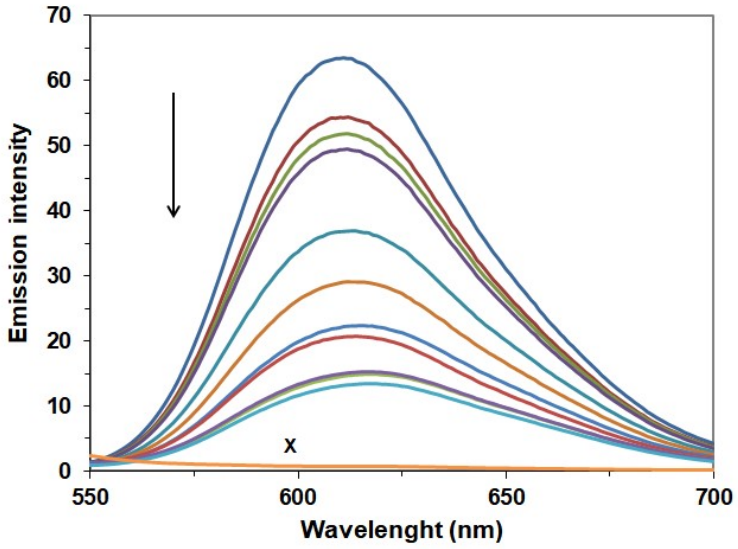

Figure S22. Emission spectra of EB bound to DNA in the presence of complex **C4**. [EB] = 2.0×10^{-5} mol dm^{-3}; [DNA] = 2.35×10^{-3} mol dm^{-3}; [complex] = 0-3.6×10^{-5} mol dm^{-3}; λ_{ex} = 520 nm. Arrow shows the emission intensity changes upon increasing complex concentration. **x** represents 3.6×10^{-5} mol dm^{-3} complex only.

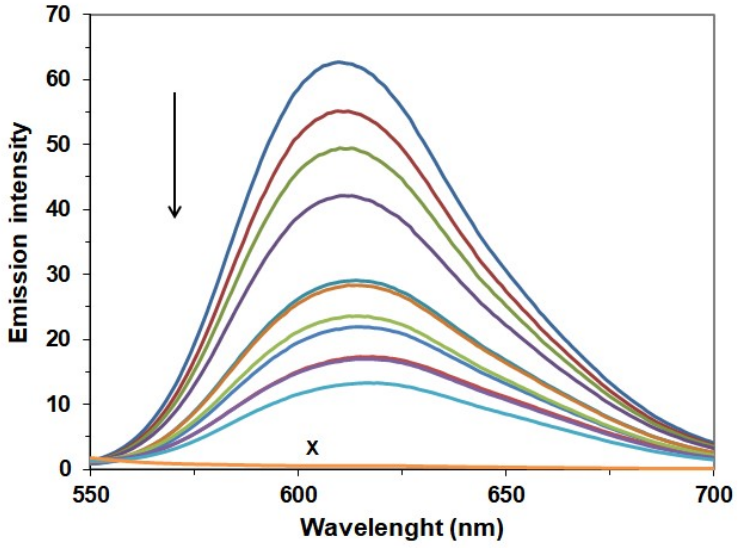

Figure S23. Emission spectra of EB bound to DNA in the presence of complex **C5**. [EB] = 2.0×10^{-5} mol dm^{-3}; [DNA] = 2.35×10^{-3} mol dm^{-3}; [complex] = 0-3.6×10^{-5} mol dm^{-3}; λ_{ex} = 520 nm. Arrow shows the emission intensity changes upon increasing complex concentration. **x** represents 3.6×10^{-5} mol dm^{-3} complex only.